

Atlantic salmon farms are a likely source of *Tenacibaculum maritimum* infection in migratory Fraser River sockeye salmon

Andrew W. Bateman, Amy K. Teffer, Arthur Bass, Tobi Ming, Karia Kaukinen, Brian P.V. Hunt, Martin Krkošek, and Kristina M. Miller

Abstract: Juvenile sockeye salmon (*Oncorhynchus nerka*) in British Columbia migrate past numerous Atlantic salmon (*Salmo salar*) farms from which they may acquire infectious agents. We analyse patterns of molecular detection in juvenile sockeye for the bacterium *Tenacibaculum maritimum*, known to cause disease in fish globally and to cause mouthrot disease in farmed Atlantic salmon in British Columbia. Our data show a clear peak in *T. maritimum* detections in the Discovery Islands region of British Columbia, where sockeye migrate close to salmon farms. Using well-established differential equation models to describe sockeye migration and bacterial infection, fit to detection data, we assessed support for multiple hypotheses describing farm- and background-origin infection. Our best models (with 99.8% empirical support) describe constant background infection pressure, except around Discovery Islands salmon farms, where farm-origin infection pressure peaked at 12.7 (approximate 95% CI: 4.5 to 31) times background levels. Given the severity of associated disease in related species and the imperilled nature of Fraser River sockeye, our results suggest the need for a more precautionary approach to managing farm-wild interactions in sockeye salmon.

Résumé : Durant leurs migrations, les jeunes saumons rouges (*Oncorhynchus nerka*) en Colombie-Britannique passent à proximité de nombreux élevages de saumons atlantiques (*Salmo salar*) qui peuvent leur transmettre des agents infectieux. Nous analysons les motifs, chez les jeunes saumons rouges, de détection moléculaire de la bactérie *Tenacibaculum maritimum*, pathogène des poissons à l'échelle planétaire qui cause la pourriture de la bouche chez les saumons atlantiques d'élevage en Colombie-Britannique. Nos données montrent une pointe très nette de détections de *T. maritimum* dans la région des îles Discovery de cette province, où les saumons rouges passent près d'élevages de saumons durant leur migration. En utilisant des modèles d'équations différentielles bien établis pour décrire la migration des saumons rouges et l'infection bactérienne, calés sur des données de détection, nous évaluons différentes hypothèses qui décrivent les infections associées aux élevages et aux conditions de référence. Les meilleurs modèles (appuyés à 99,8 % par les données empiriques) décrivent une pression d'infection de référence constante, sauf autour d'élevages de saumons des îles Discovery, où la pression d'infection associée aux élevages atteint une pointe de 12,7 fois (IC approximatif à 95 % : 4,5 à 31) les valeurs de référence. Étant donné les graves effets de la maladie associée chez des espèces apparentées et le caractère menacé des saumons rouges du fleuve Fraser, nos résultats soulignent la nécessité d'une approche plus prudente de gestion des interactions des saumons rouges sauvages avec les élevages. [Traduit par la Rédaction]

Introduction

Across taxa, long-distance migrations likely evolved to exploit resources, avoid predation, and—in some species—evade infectious disease (Altizer et al. 2011). Recent human agricultural practices, however, can result in elevated levels of infectious agents

for migratory species passing or residing nearby (Krkosek 2010; Fritzsche McKay and Hoye 2016). If left unchecked, increasing agricultural incursions into previously undeveloped spaces may lead to elevated infectious disease transmission at the wildlife-livestock interface, where human agriculture and wild species meet (Bengis et al. 2002; Wiethoelter et al. 2015). For cases in

Received 15 June 2021. Accepted 2 January 2022.

A.W. Bateman. Pacific Salmon Foundation, Vancouver, B.C., Canada; Department of Ecology and Evolutionary Biology, University of Toronto, Toronto, Ont., Canada; Salmon Coast Field Station, Echo Bay, B.C., Canada.

A.K. Teffer. Department of Environmental Conservation, University of Massachusetts Amherst, Amherst, Mass., USA.

A. Bass. Department of Forest and Conservation Sciences, The University of British Columbia, Vancouver, B.C., Canada.

T. Ming and K. Kaukinen. Pacific Biological Station, Fisheries and Oceans Canada, Nanaimo, B.C., Canada.

B.P.V. Hunt. Institute for the Oceans and Fisheries, The University of British Columbia, Vancouver, B.C., Canada; Department of Earth, Ocean and Atmospheric Sciences, The University of British Columbia, Vancouver, B.C., Canada; Hakai Institute, Heriot Bay, B.C., Canada.

M. Krkošek.* Department of Ecology and Evolutionary Biology, University of Toronto, Toronto, Ont., Canada; Salmon Coast Field Station, Echo Bay, B.C., Canada.

K.M. Miller. Department of Forest and Conservation Sciences, The University of British Columbia, Vancouver, B.C., Canada; Pacific Biological Station, Fisheries and Oceans Canada, Nanaimo, B.C., Canada.

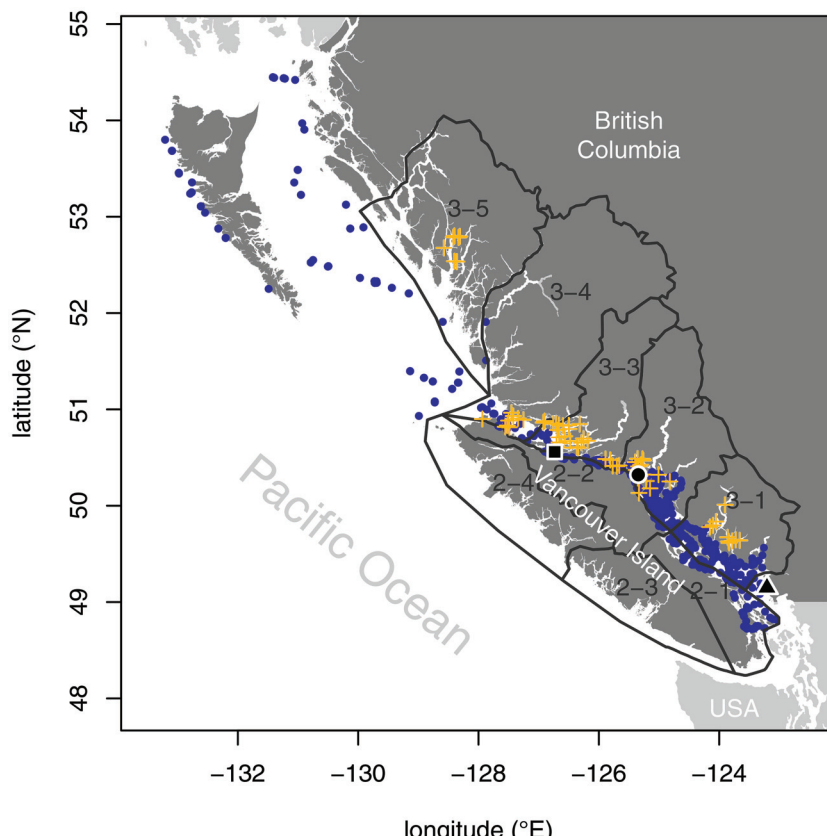
Corresponding author: Andrew W. Bateman (email: andrew.w.bateman@gmail.com).

*Martin Krkošek served as an Associate Editor at the time of manuscript review and acceptance; peer review and editorial decisions regarding this manuscript were handled by Deborah MacLatchy.

© 2022 Authors Bateman, Teffer, Bass, Hunt, and Krkošek and the Crown. This work is licensed under a [Creative Commons Attribution 4.0 International License](https://creativecommons.org/licenses/by/4.0/) (CC BY 4.0), which permits unrestricted use, distribution, and reproduction in any medium, provided the original author(s) and source are credited.

A correction was made to the e-First version of this paper on 18 May 2022 prior to the final issue publication. The current online and print versions are identical and both contain the correction.

Fig. 1. Collection locations for sockeye salmon (blue dots), along their northwestward migration after marine entry at the Fraser River mouth (black triangle), from which molecular detections of *Tenacibaculum maritimum* were analysed. Grey, labelled outlines indicate DFO's Aquaculture Management Zones, and orange crosses show the locations of relevant open-net salmon farms (within zones 3-1 through 3-5). Black circle is centred on Discovery Islands, and black square indicates northern Johnston Strait. (Map data are from Environmental Reporting BC via the *bcmaps* R package. Salmon farm locations are from DFO Aquaculture Management Division. Map projection is equirectangular.) [Colour online.]



which long-distance animal migrations intersect the wildlife–livestock interface, associated infectious diseases may place a burden on migratory species, reducing or reversing the selective advantage of migration, whether or not it originally evolved to evade infection.

Globally, farmed and wild salmon (*Salmo* spp. and *Oncorhynchus* spp.) provide a well-studied example of the wildlife–livestock interface impacting migratory species. Although most likely not in response to disease risk, salmon have evolved to migrate long distances between freshwater spawning grounds and marine feeding grounds (Maekawa and Nakano 2002). Many populations now migrate past salmon farms near points of marine entry or exit (as juveniles and adults, respectively). Farmed salmon commonly share infectious diseases with wild salmon (compare: Nekouei et al. 2018; Thakur et al. 2018; Laurin et al. 2019), and active farms may augment natural host populations to push disease dynamics over critical density thresholds and generate outbreaks (Frazer et al. 2012; Krkošek 2017). Coastal salmon farms have been implicated in disease transfer to wild populations as well as associated population declines (Ford and Myers 2008; Costello 2009). Many relevant studies have focused on the impacts of parasitic sea lice (Krkošek et al. 2011; Frazer et al. 2012; Vollset et al. 2016), and while viral and bacterial diseases remain less explored, they have long been sources concern (Hastein and Lindstad 1991; Taranger et al. 2015).

In British Columbia (hereinafter BC), one high-profile example in which livestock may impact migration is that of sockeye salmon (*Oncorhynchus nerka*) and salmon farms. Multiple populations of Fraser River sockeye salmon spawn in inland lakes and

rivers, from which juveniles migrate downstream, past open-net salmon farms in the nearshore marine environment, and then on to feeding grounds in the northeast Pacific Ocean (Groot and Margolis 1991; Connors et al. 2012). Approximately 90% of Fraser River sockeye migrate north, between Vancouver Island and the mainland of BC (Welch et al. 2011), past about half of BC's salmon farms. While time spent in the vicinity of individual farms is low (Rechisky et al. 2021), approximately 30 active farms, each farm holding 500 000 to 1 000 000 fish, lie along the main sockeye migration route between the Fraser River and the Alaska border in any given year (publicly reported data on salmon aquaculture in BC are available at <https://www.dfo-mpo.gc.ca/aquaculture/stats-eng.html>; Fig. 1). These farms can elevate the concentration of infectious agents faced by migrating juvenile sockeye (Shea et al. 2020), and depending on the agent, elevated infectivity can extend for tens of kilometres beyond the confines of a farm (Krkošek et al. 2005; Foreman et al. 2015).

Starting in about 1990, the number of maturing offspring per spawning adult (productivity) in Fraser River sockeye declined, until a record-low number of spawners returning in 2009 sparked the Cohen Commission of Inquiry into the Decline of Sockeye Salmon in the Fraser River (Cohen 2012). At a cost of over CAN\$37 million, the Cohen Commission called scores of witnesses, reviewed thousands of pieces of evidence, and ultimately made 75 recommendations to promote the recovery of Fraser River sockeye. The Commission cast particular scrutiny on the potential for disease transfer from salmon farms in the Discovery Islands region of BC (Fig. 1), where the majority of Fraser River sockeye must migrate in close

proximity to farms. A genomic signature consistent with viral disease was found to be associated with poor survival of Fraser sockeye (Miller et al. 2011), and analysis of productivity trends showed a link between Discovery Islands farm production levels and Fraser River sockeye productivity (Connors et al. 2012). A possible explanation for those trends is the transmission of infectious disease or other negative ecological interactions between farmed Atlantic salmon (*Salmo salar*) and wild sockeye salmon. Justice Cohen recommended that salmon farms in the Discovery Islands be removed if they were shown to pose any more than a minimal risk of serious harm to Fraser River sockeye (Cohen 2012). In 2020, however, assessments by the Canadian federal department of Fisheries and Oceans (DFO) concluded that nine infectious agents, considered individually, each posed a minimal risk to Fraser River sockeye as a result of potential transmission from salmon farms in the Discovery Islands (<https://www.dfo-mpo.gc.ca/cohen/iles-discovery-islands-eng.html>).

New evidence shows that one of the agents DFO assessed, *Tenacibaculum maritimum*, warrants further attention. A cosmopolitan marine bacterium that infects fish, *T. maritimum* infection does not invariably cause disease but is responsible for tenacibaculosis globally and causes “mouthrot” in Atlantic salmon on farms in BC (Frisch et al. 2018b). In a recent environmental-DNA (eDNA) study, out of 39 salmon pathogens for which presence was assessed in coastal marine waters, *T. maritimum* was one of the agents most strongly associated with active salmon farms (Shea et al. 2020). Here, we analyse new data from migrating sockeye salmon that were not included in DFO’s risk assessment (DFO 2020).

Using data pertaining to *T. maritimum* in juvenile sockeye salmon smolts originating from the Fraser River, we developed and fitted a set of empirical spatioepidemiological models to explore transmission-dynamic scenarios during the smolts’ early marine migration, from approximately April through August. Over the course of their migration, sockeye interact with many other populations of fish in addition to farmed Atlantic salmon, including other salmon species (congenerics) and Pacific herring (*Clupea pallasi*). We evaluate support for alternative hypotheses regarding farm- and background-origin infection to describe *T. maritimum* detection prevalence in sockeye smolts.

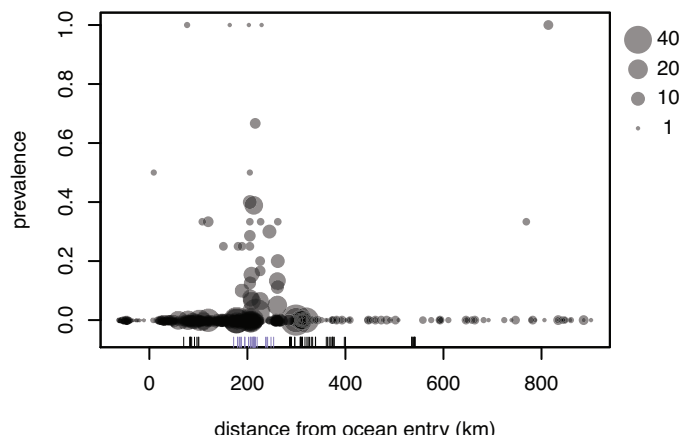
Methods

Juvenile salmon were collected under a scientific fishing permit (MECTS # 2014-502-00249) issued to Pacific Region DFO staff by the Government of Canada, DFO, Regional Director Fisheries Management. This work did not require an animal care protocol pursuant to an exemption contained in the Canadian Council on Animal Care (CCAC) guidelines applying to fish lethally sampled under government mandate for assessment purposes (4.1.2.2).

We used sockeye salmon samples and data from DFO and collaborators working on juvenile Fraser River sockeye salmon in their first year of marine residence, caught during the course of existing marine sampling programs and subsampled for pathogen and molecular analysis. Specifically, sockeye came from DFO’s trawl programs and from the Hakai Institute’s purse-seine sampling program. Our analysis includes samples collected in the spring and summer from 2008 through 2018. To evaluate evidence for infection from salmon farms versus background sources between Vancouver Island and the mainland of BC, we restricted our analyses to fish that were caught between Vancouver Island and the mainland of BC and further along the sockeye migration route to the northwest (Fig. 1), and we used genetic stock ID (Beacham et al. 2004, 2010) to further restrict our analysis to sockeye smolts from stocks known to leave the Fraser River and primarily migrate north through that region (Appendix A, Table A1).

We screened the selected sockeye for the presence of *T. maritimum* (among other infective agents) using molecular techniques described in detail elsewhere (Fringuelli et al. 2012; Miller et al. 2016). Briefly,

Fig. 2. Prevalence of *Tenacibaculum maritimum* infection, detected via high-throughput qPCR assay, in samples of Fraser River sockeye salmon smolts migrating northwestward from the mouth of the Fraser River, BC ($x = 0$). Grey circles represent smolts caught in individual trawl and purse-seine surveys between 2008 and 2018. “Rug” shows locations of salmon farm tenures, with blue indicating farms in the Discovery Islands region of BC. [Colour online.]



the methods involve nucleic acid extraction followed by quantitative polymerase chain reaction (qPCR) screening on the Fluidigm BioMark nanofluidics platform. This approach estimates specific nucleic acid sequence copy number within a fixed-volume sample at standardised nucleic acid concentration via comparison to known-concentration serial dilutions of artificial construct standards of the targeted sequence. For the purposes of our models, we reduced *T. maritimum* nucleic acid copy number data to a per-fish measure of detection. If duplicate qPCR tests on the same sample both detected the bacterium, we considered that sample to be positive; if both tests indicated a lack of the bacterium, we considered the sample negative; and if the two tests disagreed ($n = 4$), we considered the sample indeterminate and excluded it from further analyses. Resulting molecular *T. maritimum* detection data were available for 2270 Fraser River sockeye smolts.

To make the sockeye migration tractable, we simplified the two-dimensional sampling locations into measures of migration distance along a single spatial axis, representing least-seaway distance (generally to the northwest) from the Fraser River mouth. To do this, we considered all over-water straight-line paths among sample collection and shoreline points and then solved for the shortest paths between sampling locations and the Fraser River mouth using Dijkstra’s algorithm (Dijkstra 1959; Csardi and Nepusz 2006). We assigned negative migration values to sampling locations southeast of the Fraser River.

Detection data from sockeye smolt screening showed a distinct peak in *T. maritimum* prevalence near salmon farms in the Discovery Islands region of BC (Fig. 2). The vast majority of samples collected before and after the Discovery Islands, from the perspective of a migrating sockeye smolt, yielded no *T. maritimum* detections. Despite inevitable variability, samples from the vicinity of the Discovery Islands showed a pattern of substantially higher detection prevalences (Fig. A2 of Appendix A shows detailed spatial detection data in relation to salmon farms along the southern portion of the migration route).

Although it might seem natural to interpret these data as evidence that infections originating in the Discovery Islands, and the salmon farms located there, largely determine *T. maritimum* infection patterns in Fraser River sockeye salmon, we must consider several possible alternative explanations. First, any infection can take time to develop, and the spatial *T. maritimum* infection pattern may be a consequence of detections that are spatially

displaced from their precipitant exposure locations, even if infection mainly comes from largely constant background sources. Second, the pattern of infection may be best described by spatially varying background source pressure, not directly tied to salmon farms and perhaps due to idiosyncrasies of local hydrodynamic patterns (Chandler et al. 2017; Khangaonkar et al. 2017). The Discovery Islands region serves as a hydrographic funnel that concentrates all out-migrating salmon into a confined space where interactions with background infection sources may be amplified. Third, even if salmon farms are a major source of *T. maritimum* infection for Fraser River sockeye, farms in the Discovery Islands specifically may or may not provide an outsized contribution to infection pressure. In this latter case, the Discovery Islands region may be where we happen to see elevated infection rates, again due to a combination of migration and infection processes.

Our detailed analyses, described below, confronted these hypotheses, formalised as mathematical models, with the data at hand. By comparing empirical support for different models, we show which hypotheses are most consistent with observed patterns.

Model overview

We assembled models from well-established components to describe infection dynamics for Fraser River sockeye smolts as they migrated away from the mouth of the Fraser River. The partial differential equation (PDE) models we used combined two basic parts: a spatial component, to describe the changing spatial distribution of sockeye as the population migrates during a typical year, and an epidemiological component, to describe exposure to *T. maritimum*, development of associated infections, and subsequent recovery from or mortality due to those infections.

$$(1a) \quad \frac{\partial S(x, t)}{\partial t} = D \frac{\partial^2 S(x, t)}{\partial x^2} - \frac{\partial v(x)S(x, t)}{\partial x} + f(x, t) - \mu S(x, t) - S(x, t)\phi(x) + \gamma I(x, t)$$

$$(1b) \quad \frac{\partial E(x, t)}{\partial t} = D \frac{\partial^2 E(x, t)}{\partial x^2} - \frac{\partial v(x)E(x, t)}{\partial x} - \mu E(x, t) + S(x, t)\phi(x) - \rho E(x, t)$$

$$(1c) \quad \frac{\partial I(x, t)}{\partial t} = D \frac{\partial^2 I(x, t)}{\partial x^2} - \frac{\partial v(x)I(x, t)}{\partial x} - \mu_I I(x, t) + \rho E(x, t) - \gamma I(x, t)$$

(For convenience, in much of the subsequent text, we drop the explicit space- and time-dependence.) Here, S , E , and I are the space- and time-varying relative densities of susceptible, exposed, and infected individuals, respectively; x is the single spatial migration-distance dimension; t is time; D is the spatial diffusion coefficient; v is the migration speed (below, we describe how v changes in space); f represents the time-varying input of sockeye smolts at the Fraser River mouth; μ is mortality (with a different rate, μ_I , for infected individuals); ϕ represents the spatially varying cumulative infection pressure (below, we describe how this is modelled); ρ is the development rate of exposed into infected individuals; and γ is the recovery rate of infected individuals. This model form assumes that sockeye salmon can become infected with *T. maritimum* from external sources, but given the short time window during which they can be sampled, secondary transmission does not occur.

Movement model portion

To maximise our chances of being able to fit the overall model (eq. 1) to detection-prevalence data, we first parameterised the movement portion of the model (eq. A1) using additional information from a number of sources. One missing piece was an estimate for the diffusion coefficient, D . As a result, in the course of numerically solving the model (technical details below), we tuned

The spatial component of our models took the form of standard advection-diffusion equations (Murray 2007). This class of models tracks the abundance or density of individuals over space and time, in our case describing directed movement (advection) associated with migration, as well as spread (diffusion) due to variation in migration speed or milling behaviour. Technically, we modelled the spatial probability-density function for migrating sockeye that entered the marine environment in a given year. The models also capture natural mortality over the course of migration (a “decay” component). That is, the spatial density of sockeye integrates across space to a smaller and smaller fraction as some of the original total population dies as migration proceeds.

The epidemiological component of our models took a standard “susceptible-exposed-infected-susceptible” (SEIS) form, whereby the susceptible portion of the population can become exposed, after which infection develops at a given rate. This model requires modification of the spatial model by decomposing the time-varying spatial distribution of sockeye into susceptible, exposed, and infected components. Use of this epidemiological description means that the model overall must be formulated as a set of advection-diffusion-reaction equations. We assume that sockeye leave freshwater as uninfected, susceptible individuals, since *T. maritimum* is generally considered to be an obligate marine organism. Susceptible fish can become exposed due to spatially varying infection pressure in the marine environment, but we assume that molecular detection of *T. maritimum* is impossible until those exposed fish develop into infected fish. Infected fish may die at a faster rate and can recover and return to the susceptible category.

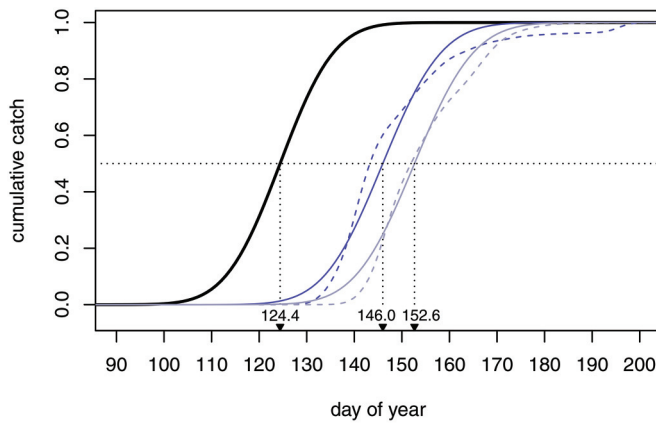
The overall model takes the following form:

D so that movement model predictions aligned with observations of migration timing at two points along the Fraser sockeye migration route.

Where information was available, we drew parameter estimates from the literature. We used the approximate long-term mean and standard deviation of sockeye smolt captures from the Mission rotary screw trap (Preikshot et al. 2012) to parameterise a Gaussian form for the input function, f . This involved a mean ordinal day of the year for smolt passage at Mission of 124 (May 4), plus a correction accounting for the distance from Mission to the Fraser River mouth of 75 km and a lower Fraser swimming speed of 187 km·day⁻¹ (Stevenson et al. 2019), and a standard deviation of nine days (Preikshot et al. 2012). We used migration speeds, v , from a tracking study of age-1 smolts (Stevenson et al. 2019), with values of 9.5 km·day⁻¹ from the Fraser River to the Discovery Islands region, and 14.5 km·day⁻¹ thereafter. We set the baseline mortality rate, μ , to 0.00924 day⁻¹ such that survival over the course of 150 days would be 25%, to approximately align with Stevenson et al. (2019). Refitting our best model (see Results) with $\mu = 0.00611$ day⁻¹, to produce 40% survival after 150 days, as seen for larger but rare age-2 smolts (Bass et al. 2020), yielded near-identical results.

We numerically solved the susceptible-only advection-diffusion-decay model in R (R Core Team 2020) using the “method of lines”,

Fig. 3. Cumulative Fraser River sockeye salmon smolt passage at Mission, BC (thick, black left-most curve, parameterised from long-term data) and in the Discovery Islands (blue middle curve; 211 km from ocean entry) and northern Johnstone Straight (grey, right-most curve; 309 km from ocean entry) regions of their northwestward migration route. For the latter two locations, solid curves come from a parameterised advection–diffusion–decay model of sockeye movement, while dashed curves show empirical data from 2015 through 2019, collected by the Hakai Institute and colleagues. Annotations indicate the day of the year at which 50% of the modelled sockeye population passes each location. [Colour online.]



as implemented in the ReacTran package (Soetaert and Meysman 2010). We used a 1 km spatial discretisation extending from $x = -100$ km (southeast of ocean entry) to $x = 1500$, and we used a 1-day temporal discretisation from ordinal days 75 (March 15) through 275 (October 2). Initial density, $S(x, 75)$, was zero, and we set zero-flux boundary conditions for x . We set the diffusion coefficient, D , by iteratively matching the modelled cumulative distribution of smolts that had passed the Discovery Islands ($x = 211$ km) and northern Johnstone Straight ($x = 309$ km; Fig. 1) to corresponding cumulative distributions of catch-per-unit-effort from purse-seine sampling run by the Hakai Institute between 2015 and 2019 (Johnson et al. 2019). Resulting model predictions from the advection–diffusion–decay movement model matched catch data well (Fig. 3).

Epidemiological model portion

Arguably the most important component of the epidemiological portion of eq. 1 is the infection pressure, ϕ , critical for drawing inference about the source of *T. maritimum* infection in juvenile sockeye. To model ϕ we considered four candidate models based on the sum of putative infection pressures from background and salmon farm sources (ϕ_B and ϕ_F , respectively): $\phi = \phi_B + \phi_F$. Two candidate submodels considered background sources only: a constant background infection pressure for all x , at level β_0 , to be determined at the time of model fitting; and background pressure that varied by DFO Fish Health Zone (Table 1), at levels β_1 , β_2 , β_3 , β_4 , and β_5 . These infection pressures were determined at the time of model fitting, via one and five free parameters, respectively. Two candidate submodels considered farm-source infection in addition to constant background pressure: one accounted for farm activity and distance from farms, and the other modified the first, allowing farms in the Discovery Islands to contribute proportionately more or less to overall farm-source infection pressure.

The first farm-source infection submodel considered infection risk that declined with distance from each active farm according to a Gaussian “dispersal” kernel, assuming an average source strength proportional to total months of farm activity in our study period. We used a Gaussian kernel as a coarse phenomenological

Table 1. Migration-distance cutoffs used in spatioepidemiological models to approximate DFO Aquaculture Management Fish Health Zones along the northwestward migration of juvenile Fraser River sockeye salmon.

Fish Health Zone	Southern boundary (km)	Northern boundary (km)
3-1 and south	—	130
3-2	130	234
3-3	234	343
3-4	343	410
3-5 and north	410	—

Note: Boundary locations were generated by comparing migration distance (x) estimates at sockeye sampling locations to known zonal boundaries.

description of bacterial dispersal around a farm, reasoning that the cumulative infection pressure from multiple farms would likely have more bearing than the kernel’s particular functional form. Scaling source strength to proportional farm activity (Salama and Murray 2011) effectively modelled infection pressure at a typical point in time, since we deemed that data constraints made a complex time-varying model of infection pressure infeasible for overall model fitting. The per-farm contribution to infection pressure took the following form:

$$(2) \quad \phi_{F,i}(x) = \sum_{\text{all } j} \frac{A(i,j)}{\sigma \sqrt{2\pi}} e^{-\frac{1}{2}(d_i(x))^2 / \sigma^2}$$

where $A(i,j)$ is an indicator function that is one if farm i was active in month j and zero otherwise, σ is the standard deviation of the kernel to be determined at the time of model fitting, and $d_i(x)$ is a distance function for each farm. The $d_i(x)$ terms account for the facts that migrating sockeye approach and then pass each farm along their migration route, but many farms do not lie directly on that route. We empirically approximated each farm’s $d_i(x)$ by fitting a shifted absolute value function of migration distance (x) to seaway distances from farm i to the sampling location of each sampled fish (e.g., Appendix A, Fig. A3). Each $d_i(x)$ function had parameters for the minimum value, a_i , and x value at that minimum, $x_{0,i}$, and was fit assuming normally distributed residuals with standard deviation $\sigma_{d,i}$. The final version of the farm infection pressure was the scaled sum, across all farms, of the per-farm contribution in eq. 2. Further, although we simplified our modelling framework to consider only a single spatial axis, x , the real population of migrating fish is spread out perpendicular to our migration axis. To account for variation in the distance to each farm, as experienced across the population at each migration distance, we averaged across the residual variation from our $d_i(x)$ fits (i.e., the distribution of distance to farm i for fish caught at location x), so that

$$(3) \quad \phi_F(x) = \frac{\beta_F}{K_{F0}} \sum_{\text{all } i} \int_{-a_i}^{\infty} g(y | \sigma_{d,i}) \phi_{F,i}(x+y) dy$$

where β_F is a scaling parameter also to be determined at the time of fitting, K_{F0} is a standardisation factor (the maximum value of the sum to the right, over all x), $g(y | \sigma_{d,i})$ is the Gaussian probability density function with standard deviation $\sigma_{d,i}$ and mean 0 evaluated at y . The lower limit of the integral is set to avoid considering non-sensical negative farm distance values at $x_{0,i}$, where migrating individuals come closest to the farm and the highest associated infection pressures will occur. The K_{F0} factor ensures that β_F is the maximum value of ϕ_F , for ease of comparison to ϕ_B . In practice, to facilitate repeated calculation during model fitting, we approximated ϕ_F by replacing the integral in eq. 3 with a Riemann sum

Table 2. Comparison of fitted spatioepidemiological candidate models to describe patterns of *Tenacibaculum maritimum* detection in Fraser River sockeye salmon smolts during their early marine migration.

Model	Epidemiological form	Infection submodel	Fitted parameters	-log(\mathcal{L})	ΔAIC	Akaike weight
1	SIS	Constant background infection	3	269.5	29.3	0.0%
2	SIS	Zonal background infection	7	258.3	15.0	0.0%
3	SIS	Background & farm infection	5	261.0	16.3	0.0%
4	SIS	Background and farm infection, separate DI source strength	6	252.3	1.9	28.1%
5	SEIS	Constant background infection	4	268.7	29.8	0.0%
6	SEIS	Zonal background infection	8	256.1	12.5	0.1%
7	SEIS	Background and farm infection	6	260.6	17.5	0.0%
8	SEIS	Background and farm infection, separate DI source strength	7	250.8	0.0	71.7%

Note: SIS, susceptible infected susceptible; SEIS, susceptible exposed infected susceptible; DI, Discovery Islands.

from $-3\sigma_{d,i}$ (or $-a_i$, whichever was greater) to $3\sigma_{d,i}$ with 0.1 km intervals. To manage numerical errors, we also imposed a lower bound of 0.1 km on σ (the standard deviation of the infection kernel) so that any infection kernel was not “skipped over” by too coarse a discretisation.

The second version of the farm-source infection submodel allowed for different source strengths for Discovery Island farms relative to other farms along the sockeye migration route. While this model form may seem unduly bespoke to represent an a priori hypothesis, it was informed by past focus on salmon farms in the Discovery Islands, in particular, as sources of infection that might place Fraser River sockeye at risk (Cohen 2012). To achieve this, we replaced $A(i, j)$ in eq. 2, where i corresponded to Discovery Island farms, with $e^\delta A(i, j)$. Here, e^δ is a scaling factor, with $\delta > 0$ leading to elevated (and $\delta < 0$ leading to reduced) infection pressure from Discovery Island farms.

For all versions of the epidemiological submodel, we considered the development rate ($\rho > 0$) and recovery rate ($\gamma > 0$) to be free parameters, determined at the time of model fitting, and we modelled infected mortality as a scaled version of baseline mortality: $\mu_I = e^\eta \mu$. Here, e^η is an inflation factor ($\eta > 0$ assumed, also treated as a free parameter) that controls mortality in infected individuals, relative to background mortality.

Model fitting and comparison

We treated the parameterised movement portion of the model as fixed, given the quality of data we used for parameterisation. We also assumed movement parameters to be the same for each epidemiological class of fish in eq. 1. This allowed us to focus model fitting on unknown parameters related to infection pressure(s) and progress.

In fitting the epidemiological components of the model to the *T. maritimum* detection data from sockeye smolts, we used the same approach to numerically solve eq. 1 as we had for the movement model (eq. A1) alone. Assuming that molecular detections were from infected fish only, we took the infection status of each fish, k , sampled at location $x(k)$ and time $t(k)$, to have come from a Bernoulli distribution with probability of infection:

$$(4) \quad P(k) = \frac{I[x(k), t(k)]}{S[x(k), t(k)] + E[x(k), t(k)] + I[x(k), t(k)]}$$

Thus, the likelihood for the infection status of fish k was $\mathcal{L}_k = P(k)$, if *T. maritimum* was detected, and $1 - P(k)$ otherwise. In fitting the model, we minimised the negative log of \mathcal{L} , the joint likelihood across all screened sockeye salmon. Assuming independence among observations, this was

$$(5) \quad -\log(\mathcal{L}) = \sum_{\text{all } k} -\log(\mathcal{L}_k)$$

We minimised eq. 5 with R’s optim numerical optimiser, using the Nelder–Mead algorithm to find the combination of model

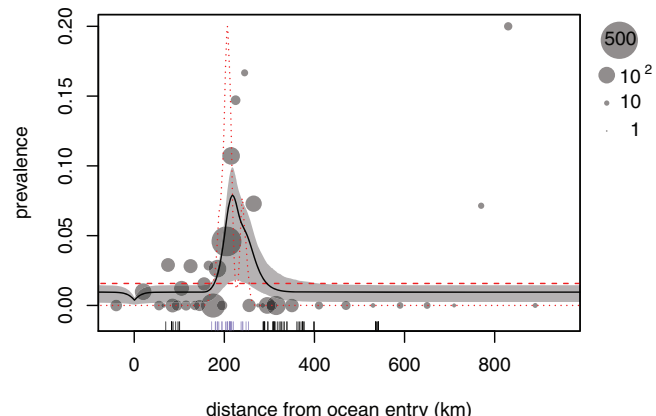
parameters that minimised each model’s negative log-likelihood, given the data. That is, we solved for the maximum-likelihood estimates (MLEs) of the parameters. For each of the four infection submodels, we considered both a SEIS version of the partial differential equation model (eq. 1) and a slightly less complex “SIS” version (susceptible–infected–susceptible), in which exposed individuals immediately become infected, without passing through a separate exposed class. Overall, this meant that we fit eight candidate models: an SEIS and SIS version with each of four infection submodels (Table 2).

For each model, we calculated Akaike’s information criterion (Akaike 1973) and ΔAIC scores (difference in AIC relative to the lowest AIC model). Lower ΔAIC values indicate “better” (more parsimonious) models, with values below two indicating substantial model support, values above four indicating considerably less support, and values above ten indicating essentially no support (Burnham and Anderson 2002). Associated Akaike weights represent the strength of evidence for each model, given the candidate model set.

Parameter and model uncertainty

We initially attempted to estimate parameter confidence intervals via the quadratic-approximation method (Bolker 2008). The scaling parameter for the Discovery Island farm infection strength, δ , caused problems, however; the Hessian (second-derivative “curvature” matrix) of the negative log-likelihood function, evaluated at the MLEs, could not be inverted to yield the approximate variance–covariance matrix for the parameter estimates (Bolker 2008). As a result, we used likelihood profiles, fixing one or two parameters at a sequence of values spanning their MLEs and optimising all other parameters to explore the likelihood function. We first generated a likelihood profile and associated confidence interval for the δ parameter, which indicated that large values of δ all produced an effectively equivalent model fit (explaining the uninvertible Hessian; Appendix A, Fig. A7A). In light of this result, to improve the stability of the optimiser and allow estimation of a variance–covariance matrix for the remaining model parameters, we used a Discovery Island-only version of the farm infection submodel, ϕ_F , for further uncertainty calculations. That is, we set farm contributions outside of Fish Health Zone 3–2 (Table 1) to zero. Our resulting confidence estimates may thus be slightly too small (since a variable δ could improve the model fit at each combination of the other parameters); however, given the clear results with respect to δ , we deemed it useful to present uncertainty estimates, approximate though they are. Using the δ -restricted model, we generated a likelihood profile and associated confidence interval for σ , the parameter controlling the spread of infection around individual farms. We also generated joint likelihood profiles and associated confidence regions for (1) the infection parameters (β_0 and β_F) and (2) the infected mortality (μ_I) and recovery (γ) parameters.

Fig. 4. Prevalence of *Tenacibaculum maritimum* infection in Fraser River sockeye salmon smolts migrating northwestward from the mouth of the Fraser River, BC ($x = 0$). Grey circles represent smolts caught in trawl surveys and purse-seine sampling between 2008 and 2018 (aggregated by location to illustrate pattern). Black curve shows predictions from a spatioepidemiological model of migration and infection dynamics, fitted to the prevalence data and plotted for the average ordinal day of fish capture; surrounding light grey shows 95% confidence region, for model incorporating background and Discovery Island farm infection sources. Red curves show model-fit relative infection pressure from background (dashed) and salmon farm-origin (dotted) sources, primarily in and around the Discovery Islands (scale arbitrary). “Rug” shows location of salmon farm tenures, with blue indicating Discovery Islands farms. [Colour online.]



To generate confidence regions for predictions from the best model (subject to the Discovery Island-only modification to improve numerical stability), we drew 1000 samples from a multivariate normal distribution with means equal to the MLEs and variance-covariance matrix estimated from the curvature of the negative log likelihood at the MLEs. For each of these parameter combinations, we generated model predictions, and at each spatiotemporal location (x, t) we generated desired percentiles, representing the specified range of uncertainty associated with the fitted model.

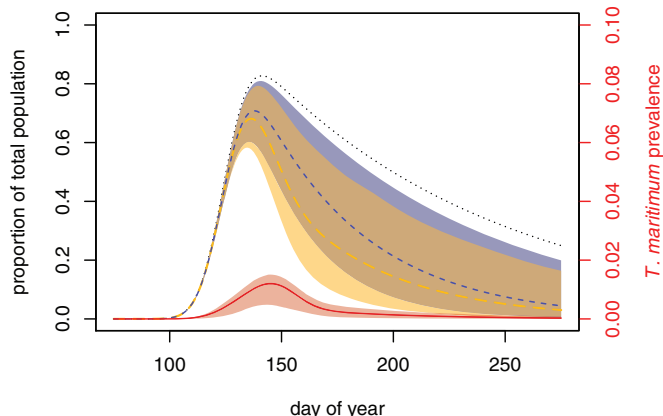
Interannual variation

We base inference on models fit to data from all years of our study. In part, this was due to a lack of comprehensive data (e.g., incomplete annual migration-timing data at Mission, inconsistent relative abundance measures along the sockeye migration route). Interannual variation in infection rates does, however, occur. In 2015, in particular, we saw high *T. maritimum* infection rates in Fraser River sockeye smolts in the marine environment. To explore how this might have affected our conclusions, we refit the best version of the epidemiological submodel using data from 2015 alone and to data from all other study years. In both cases, *T. maritimum* detection data and farm-stocking data were specific to each time period.

Results

The best partial differential equation model of *T. maritimum* infection prevalence in juvenile Fraser River sockeye was the SEIS version in which farm-source infection differed between Discovery Islands and other farms (Model 8; Table 2). This model accounted for 71.7% of model support, and when considered along with the corresponding SIS model (Model 4; Table 2), the associated version of the infection submodel accounted for 99.8% of model support. The best model described a pattern of infection prevalence that was relatively constant throughout the sockeye migration route, except around Discovery Island farms, where infection was elevated (Fig. 4). While the movement model described

Fig. 5. Spatioepidemiological model predictions of proportional Fraser River sockeye salmon smolt marine abundance (black, left side of panel) by day of the year, assuming (1) background-only mortality (dotted curve), (2) mortality due to background *Tenacibaculum maritimum* infection (dashed blue curve and 95% confidence region), and (3) mortality due to background and farm-origin *T. maritimum* infection (long dashed orange curve and 95% confidence region). Sockeye enter from fresh water over time but immediately incur some level of mortality, such that the whole population is never in saltwater at once and proportional abundance never reaches 1. Red curve (and 95% confidence region) indicates *T. maritimum* infection prevalence in model 2 (note different scale). [Colour online.]



a wave of sockeye population density travelling north (Fig. 3, Appendix Fig. A1A), the spatial pattern of infection prevalence changed little over the course of the migration season (Appendix Fig. A1B). These patterns combined to produce a peak in population-wide infection prevalence just before ordinal day 150 (May 30), as most sockeye passed the Discovery Islands (Fig. 5).

The best model describes a scenario in which sockeye salmon smolts are subject to *T. maritimum* infection from both background and salmon farm sources. Peak contributions from Discovery Island farms dwarfed those from other farming locations, and farm-source infection pressure peaked at 12.7 times background infection pressure. Despite this higher estimated peak exposure due to salmon farms, cumulative exposure along the migration route was higher for background sources. Numerically integrating background- and farm-source exposure rates across the migration window, farm-origin exposure occurred, over approximately a 100 km portion of the migration route, in approximately 0.21 of the modelled sockeye population. Background-origin exposure occurred in 0.43 of the sockeye population, over the entire 1600 km spatial window we modelled. (Note that some repeat exposure is possible due to recovery in the model.) The MLE parameters resulted in 67.7% survival (95% CI: 43.9% to 93.5%) by the end of the migration period, relative to survival that would result in the context of background infection only (Fig. 5). That is, between 6.5% and 56.1% of sockeye smolts appear to die as a result of farm-origin *T. maritimum* exposure. (Note that confidence regions for survival in the full model and the background-only model (Fig. 5) appear to overlap, but these rates are not independent; survival in the full model at most equals background-only survival.)

Model uncertainty

Although there was substantial uncertainty in parameters from our best model, results indicated several clear features relevant for Fraser River sockeye. The exponent for Discovery Island farm infection scaling factor, δ , was clearly greater than zero (Appendix Fig. A7A) with a lower 95% confidence bound of 1.53, yielding a lower 95% confidence bound on the scaling factor itself, e^δ , of 4.6. The best-fit value for e^δ was 8.8×10^4 , however, and

the likelihood appeared to decline monotonically with increasing δ . The standard deviation parameter for salmon farm-origin infection pressure, σ , was estimated to be near the minimum permitted value of 0.1 (Appendix Figs. A7B, A4), with an upper 95% confidence bound of 12.8. A wide range of mortality (μ_i) and recovery (γ) values produced similar model fits (Appendix Fig. A7C), with the model unable to discern whether infected mortality was elevated, relative to baseline mortality, or whether infected individuals recovered at a non-zero rate.

Background- and peak farm-origin and infection rates (β_0 and β_F , respectively) also displayed a wide range of likely values (Appendix Fig. A7D), but the estimates indicate that farm-source infection pressure was 12.7 times background levels with a 95% confidence region that spanned 4.5 to 31 times background levels.

Even though infection, recovery, and associated mortality parameters were not simultaneously estimable, given the data, the resulting model showed a well-resolved peak in *T. maritimum* prevalence near Discovery Island salmon farms (Fig. 4). The model form used to estimate uncertainty illustrated in Fig. 4, however, considered only Discovery Island salmon farms due to optimisation constraints. Appendix Fig. A5 shows model predictions from the best-fit version of our most parsimonious model form (Model 8 from Table 2) with δ fixed at 1.53, the lower bound of its 95% confidence interval. Despite lingering uncertainty in the particulars of our best model, the influence of Discovery Islands farms stands out as receiving the overwhelming majority of model support across the models we considered (Table 2).

Interannual variation

Tenacibaculum maritimum prevalence was high in 2015, and our best model, fit to data from that year alone, was consistent with much higher levels of background- and farm-origin infection than the model fit to data from all other years (Fig. 6A). The fitted model for 2015 indicates more even contributions from salmon farms along the sockeye migration route, due to higher rates of *T. maritimum* detection in fish caught further to the south. Unfortunately, sampling was spatially restricted in 2015, precluding validation of the putative pattern using samples from further north. Regardless, the infection peak associated with Discovery Island farms did not disappear when 2015 data were omitted from those used to fit the model, although that peak was substantially lower (Fig. 6B).

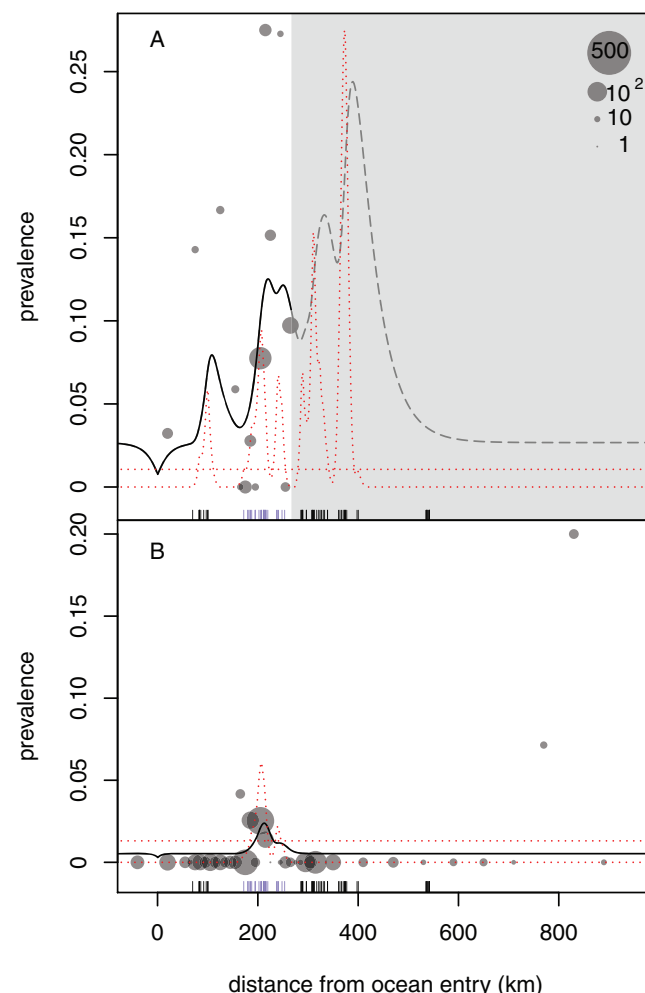
Information from salmon farms

Using our best model as a starting point, we considered two further model modifications, based on information from salmon farms.

First, *T. maritimum* in Atlantic salmon in BC tends to cause acute disease from which individuals can recover, not commonly displaying signs of disease again (DFO 2020). As a result, we fit an "SEIR" (susceptible–exposed–infected–recovered) version of the best model, which allows for a new recovered class relative to the SIS and SEIS models. The likelihood was within 0.02 of the best-fitting model, with an equal number of parameters, presenting a nearly identical model fit (Appendix Fig. A6). This result was consistent with our uncertainty calculations, which indicated that the modelling framework cannot resolve the details of recovery from infection (Appendix Fig. A7C).

While farmed salmon do not tend to experience recurrent mouthrot, the initial bout on a farm can lead to substantial mortality, and fish are treated with antibiotics (Frisch et al. 2018b). Treatment with appropriate antibiotics may therefore be an indicator of farm outbreaks during which *T. maritimum* release would be elevated (Z. Waddington and D. Price, personal communication 2020). We considered an additional modification to the best-fitting model, scaling treated farms' contributions to farm-source infection pressure (eq. 2) by an additional free parameter in the months during which they were treated. Thus, farms that were

Fig. 6. Prevalence of *Tenacibaculum maritimum* infection in Fraser River sockeye smolts migrating northwest from the Fraser River, BC ($x = 0$), for 2015 (A) and for all other study years from 2008 through 2018 (B). Grey circles represent smolts caught in trawl surveys and purse-seine sampling, aggregated by location to illustrate pattern. Black curves show predictions from spatioepidemiological partial differential equation models of migration and infection dynamics, fitted to the relevant prevalence data and plotted for the average ordinal day of fish capture. Model curve in panel A is dashed and background is shaded where detection data are lacking. Red dotted lines show relative infection pressure from fitted constant and salmon farm-origin sources in the corresponding time periods (scale arbitrary but matching in A and B). "Rug" shows location of salmon farm tenures, with blue indicating Discovery Islands. [Colour online.]



treated more often during the study period had the potential to contribute more to farm-source infection pressure. This model did not significantly improve the model fit (likelihood ratio test, $p = 0.36$).

Discussion

Fraser River sockeye smolts, migrating northwest after ocean entry, displayed a sharp peak in *T. maritimum* detections in the Discovery Islands region of BC, about 200 km after they had left fresh water (Fig. 2). Standard differential equation models fit to these data indicate that Atlantic salmon farms in the Discovery Islands

likely contribute to *T. maritimum* infection rates in Fraser River sockeye. An advection–diffusion–decay submodel, parameterised with data from multiple sources, described sockeye migration north from the Fraser River, and we fit competing SEIS (susceptible–exposed–infected–susceptible) submodels to qPCR molecular-detection data to describe the epidemiology of *T. maritimum* in sockeye. Our best models, fitted to the available data, described a peak in farm-source infection rates that was an order of magnitude (12.7 times) higher than background infection rates. Farm-origin infection in sockeye occurred over a short portion of the early marine migration route, but at such high intensity that total farm-origin infections approached total background-origin infections acquired over the entire migration route.

There was substantial interannual variation in the prevalence of *T. maritimum* detections, with almost three quarters of detections seen in a single year, 2015. Although the pattern of elevated detections around Discovery Island salmon farms held up in 2015 and in the other ten years combined, detections were more common at all locations in 2015. Further, the spatial extent of sampling was restricted in 2015 such that all samples were collected within 300 km of the Fraser River mouth, and two anomalously high-prevalence samples were collected roughly 200 km north of the most northerly farms in 2012. These features of the data contribute to uncertainty and increase potential bias in our overall results, especially if actual spatial patterns in 2015 deviated from our fitted model description. Clearly, there are aspects of the system that our model does not capture, and further investigation of interannual and spatial patterns seems warranted.

Using the data that were available, uncertainty in the model parameters left ambiguity around several features of interest, but the fitted models nevertheless allowed inference and produced reasonably precise spatiotemporal predictions (but see note about uncertainty and potential bias, above). In particular, we could not make high-precision estimates for a number of parameters on their own, and we focused on the inference we could draw from these parameters, whether working alone or in combination. The uncertain parameters included the weighting of infection pressure from Discovery Island farms relative to other farms along the sockeye migration route, specific infection rates from farm and background sources, and recovery and mortality rates in infected fish (Appendix Fig. A7). Due to the specific mathematical formulation of our model, the most we can say about Discovery Island farm weighting is that it was high, describing a scenario in which farm-source *T. maritimum* infection pressure from Discovery Island far exceeded that from other farms. In the case of farm- versus background-origin infection rates, the individual parameter values were uncertain, but results indicate that peak farm-source infection pressure was between 4.5 and 31 times as high as average background infection pressure (Appendix Fig. A7D). The question of whether infection prevalence declines due to mortality or recovery was particularly unclear, even though the maximum-likelihood parameter values describe a scenario in which most of the decline in prevalence was due to mortality. Regardless of uncertainties, the range of parameter values supported by the data all led to the same overall conclusions: at its peak, infection pressure from farm-origin sources appears to have been many times stronger than that from background-origin sources, and the main peak of infection occurred near the cluster of farms in the Discovery Islands.

The fitted model indicates that *T. maritimum* infection can be detected shortly after farm-source exposure, resulting in peak infection close to salmon farms in the Discovery Islands (Fig. 4). Although this progression from exposure to detectable infection seems rapid, the timeline aligns with evidence from Atlantic salmon farms, which suggests that *T. maritimum* infection, disease development, and resulting mortality in untreated fish can be swift, with associated deaths observed as early as two days after transfer to saltwater (Frisch 2018). Even though evidence from another species

cannot validate our sockeye model, *per se*, our model's consistency with observations in another salmonid is reassuring. Known, rapid migration times for juvenile sockeye through the Discovery Islands (generally between two days and two weeks; Rechisky et al. 2021) further align with the description of directed migration in our model. In reality, there are multiple routes that smolts take through the Discovery Islands (Rechisky et al. 2021), but our model, which spatially simplifies sockeye movement into a single north–south migration axis, aims to capture broad patterns and cannot hope to capture the details of migration routes and variable exposure to infection through a complex archipelago (Rechisky et al. 2021). Nonetheless, an ability to rapidly detect *T. maritimum* in sockeye after they were exposed, paired with the smolts' broadly directional migration behaviour, appears to have facilitated identification of infection sources.

We note that the sockeye smolts we classified as infected may combine truly infected individuals with those merely exposed to *T. maritimum* at high loads. After such exposure, bacteria adhering to an individual's gills, but not truly infecting the fish, might have been detected in our mixed-tissue screening procedure. Scepticism has been levelled at past uses of gill-inclusive mixed-tissue samples for screening on the Fluidigm BioMark platform (A. Bateman, personal communication, various sources). Gills are, however, one of the tissues in which mouthrot manifests in Atlantic salmon (Frisch et al. 2018b), infections can become systemic (Frisch et al. 2018a), and our own assessments of single-tissue results (not shown) indicate that detections are indeed often systemic, especially when nucleic acid copy numbers are high. We cannot exclude the possibility that the rapid increase in and subsequent decline of *T. maritimum* prevalence near Discovery Island farms may be due to misclassification of exposure as infection, with "recovery" simply due to elution of bacteria into the marine environment. Regardless, Fraser River sockeye infected with or exposed to *T. maritimum* are most prevalent near salmon farms in the Discovery Islands, implying that those farms are — at a minimum — likely sources of exposure.

While we cannot attribute specific *T. maritimum*-induced mortality rates based on our analysis, elevated infection-induced mortality rates do align with other sources of information. In addition to the rapid mortality observed in farmed Atlantic salmon (Frisch 2018), mortality of lab-reared Atlantic salmon smolts cohabiting with artificially infected individuals has reached as high as 100% in ten days, for certain isolates of *T. maritimum* (Frisch et al. 2018b). Although a certain level of virulence in one host species does not directly imply similar virulence in another, it seems that a high rate of *T. maritimum*-induced mortality in affected sockeye would be reasonable to expect, especially considering that wild sockeye smolts are subject to additional foraging and predator-avoidance burdens, not present for farmed or lab-reared fish (Bakke and Harris 1998; Miller et al. 2014; DFO 2020), and that the region of peak infection imposes particular foraging constraints on salmon smolts (McKinnell et al. 2014; James et al. 2020). That said, our maximum-likelihood estimate of infection-induced mortality is likely too high, since resulting survival at the end of our roughly five-month migration window fell to 3.0% (95% CI: 0.2% to 16.4%), a level comparable to overall lifetime marine survival estimated for sockeye salmon (e.g., Irvine and Akenhead 2013).

Even without a definitive estimate of infection-induced mortality rates, our model results clearly illustrate the general point that infection prevalence need not be high to cause substantial mortality. The best-fit model parameters indicate a high mortality rate and relatively low recovery rate in infected individuals (Appendix Fig. A7C), combining to reproduce the observed decline in infection prevalence as sockeye smolts migrated past the Discovery Islands (Fig. 4). The resulting predicted mortality due to *T. maritimum* was 87.9% by ordinal day 275 (150 days after mean ocean-entry date), even though population-wide infection prevalence peaked at just 1.2% around ordinal day 150 (25 days after ocean entry). Although

the fitted model indicates that many fish became infected, they either died as a result or recovered so that population-wide infection prevalence at any single point in time remained low. Apparent low-prevalence infections can belie high resultant mortality.

Our best-fitting model's counter-intuitive mismatch between low overall infection prevalence and high associated mortality is, in part, a result of external-source infection pressure, whereby the modelled sockeye population itself did not have to sustain and transmit the infection internally. On reflection, we should perhaps not expect high infection prevalence for a virulent pathogen in an impacted wild population if infections primarily derive from a stable external infection source. In general, direct disease-induced mortality can be rapid for some pathogens (e.g., Frisch et al. 2018b), and diseased individuals may suffer indirect mortality through their inability to find food or evade predators (Bakke and Harris 1998; Miller et al. 2014; James et al. 2020; Furey et al. 2021). As a result, infected individuals may drop out of a population without spending much time infected, keeping the overall proportion of infected individuals at any one time low. A key point here is that the pathogen does not have to sustain itself in the wild population if a nearby stable infection source is present. Outbreaks that would normally "burn out" in the wild have the potential to persist in the system overall, and wild populations can be driven to extinction (de Castro and Bolker 2004). In the case of parasitic infections, this phenomenon has been described as an induced Allee effect that reservoir hosts can impose on endangered wildlife (Krkošek et al. 2013). There is no guarantee that any given rare pathogen will have a large effect, but in the scenario we describe, a pathogen need not be common in a focal population to cause substantial losses. The data we analysed here are consistent with an effect in sockeye due to *T. maritimum* from Atlantic salmon farms that is disproportionate to the observed prevalence.

Persistent infection on salmon farms

Longitudinal data from salmon farms in BC indicate that Atlantic salmon can remain infected or become reinfected with *T. maritimum* throughout an 18-month production cycle (Bateman et al. 2021), but Atlantic salmon rarely, if ever, develop clinical mouthrot twice (Z. Waddington and D. Price, DFO Aquaculture Management veterinary staff, personal communication, 2020). Not knowing how infection plays out in sockeye, we considered a "SEIR" version of our best-fitting model that included a "recovered" class of individuals that could not become reinfected. Results and model fit were practically identical to those of our most parsimonious model (Appendix Fig. A6). This finding aligns with the conclusion that our modelling framework cannot distinguish between recovery and mortality that both serve to reduce infection prevalence. Such a result is common in epidemiological studies, and more detailed data on recovery versus mortality arising from direct and indirect ecological processes are needed.

While antibiotic treatment is almost certainly related to disease state in farmed fish, our lack of evidence for a treatment effect on farm infection pressure aligns with observations about *T. maritimum* from other studies (Laurin et al. 2019; Shea et al. 2020). In preliminary analyses (results not shown), we found no association between farm treatment status and either *T. maritimum* detection prevalence in fish sampled as part of DFO's audit program or *T. maritimum* detections via eDNA sampling in the nearby marine environment. Further, although on-farm antibiotic treatment can extend for several months (Z. Waddington and D. Price, personal communication, 2020), dead and dying fish on farms can display elevated *T. maritimum* detection loads for somewhat longer, after any reported mouthrot outbreak has passed (Bateman et al. 2021). Together, these results suggest that antibiotic treatment, infection status, and possibly infectivity may not be intimately tied. Thus, farmed salmon infected with *T. maritimum* may continue to pose a risk to wild salmon even after the associated disease is brought under control on a farm.

Environmental effects

Environmental features we did not consider likely contribute to some of the patterns we observed. We have not taken detailed ocean circulation patterns into account, although circulation models do not suggest that the Discovery Islands represent a region of unexpected pathogen retention (Foreman et al. 2015; Khangonkar et al. 2017). The Discovery Islands region does, however, act as a funnel for out-migrating juvenile sockeye as they leave the wider reaches of the Salish Sea to the south. This concentrates sockeye smolts in a confined space within which interactions with wild species may be amplified. *Tenacibaculum maritimum* is present in cnidarian species in other parts of the world (Delannoy et al. 2011), although the extent to which this occurs in BC is unknown. Other authors have considered infection in Pacific herring (Marty et al. 2010), observed to school with juvenile sockeye at times (Johnson et al. 2019), but screening within our lab (K. Miller, unpublished results) detected mostly low levels in just eleven out of 378 Pacific herring samples. The bacterium is certainly present in other wild Pacific salmon (K. Miller, unpublished data), which can also school with sockeye and may constitute an additional source of exposure.

Another plausible explanation for the patterns we observed is the spatial patterning of environmental stressors that render fish more susceptible to disease caused by *T. maritimum* (Santos et al. 2019). Water temperatures in eastern parts of the Discovery Islands, and especially in the Salish Sea further to the south, tend to be high relative to surrounding regions (Chandler et al. 2017). This may cause thermal stress in migrating smolts. Sockeye may also start to experience food stress as they pass through the Discovery Islands (McKinnell et al. 2014; James et al. 2020), which could in turn facilitate opportunistic *T. maritimum* infection. Rather than discount salmon farms in the Discovery Islands as sources of exposure, however, nearby sources of environmental stress may help to explain why those farms, and not farms from other regions, appear to have contributed disproportionately to infection patterns.

The particularly prevalent *T. maritimum* detections in 2015 corresponded to a year of anomalously high ocean temperatures (Kintisch 2015). This further corresponded to particularly poor marine survival for the Fraser sockeye that migrated to sea that year and returned to spawn in 2017 (Hawkshaw et al. 2020). Ocean temperatures themselves are inversely related to sockeye marine survival, however (Hawkshaw et al. 2020), and *T. maritimum*, sometimes described as an "opportunistic" pathogen (Avendaño-Herrera et al. 2006), may be an indicator of other determinants of poor survival in smolts. Still, given its relatively high thermal optimum (30 °C; Avendaño-Herrera et al. 2006), we might expect to see more *T. maritimum*-related issues for salmon farms and wild species alike as ocean temperatures warm over the coming decades.

Conservation implications

Overall, it is clear that detections of *T. maritimum* in Fraser River sockeye smolts are substantially elevated surrounding an intensive salmon-farming region of BC, the Discovery Islands. Salmon farms in this area have been the subject of intense scrutiny for over a decade, largely because of the potential disease risks they pose to sockeye and other wild salmon (Connors et al. 2012; Morton and Routledge 2016). The models and data we present are consistent with combined farm- and background-source *T. maritimum* infection and associated mortality in Fraser River sockeye. Salmon farms have long been tied, globally, to sympatric declines in wild salmonids (Ford and Myers 2008), and our analysis provides an in-depth case study that builds on previous high-level correlative investigation of Fraser River sockeye salmon survival in relation to salmon farm production in the Discovery Islands (Connors et al. 2012).

Scientific advice recently provided to Canadian policymakers identified *T. maritimum* as posing minimal risk to Fraser River sockeye (DFO 2020). That assessment, however, did not access many of

the data we used here, which indicate a spatial association between *T. maritimum* infection of juvenile sockeye salmon and salmon farms in the Discovery Islands. Taken together, results from our wild salmon screening program highlight *T. maritimum* transmission as a possible mechanism for population-level impacts of farmed Atlantic salmon on wild Pacific salmon populations in BC and present evidence that elevated infections in Fraser River sockeye likely originated from salmon farm sources in the Discovery Islands region. These findings, paired with the continued declines in sockeye population health (COSEWIC 2017; Hawkshaw et al. 2020), suggest that recent conclusions about the “minimal risk” of harm posed by this agent (DFO 2020) were premature.

During preparation of this study, the Government of Canada announced a decision to remove open-net salmon farms from the Discovery Islands region of BC (<https://www.canada.ca/en/fisheries-oceans/news/2020/12/government-of-canada-moves-to-phase-out-salmon-farming-licences-in-discovery-islands-following-consultations-with-first-nations.html>). While this decision was made on the basis of consultations with local Indigenous title holders, rather than risks posed by salmon aquaculture per se, our findings suggest that the decision was nonetheless precautionary in effect, when viewed from the perspective of conserving Fraser River sockeye salmon.

Broader conclusions

Sockeye salmon are just one example of the many migratory species that globally travel large distances to complete their life cycles. Humanity’s footprint on planet Earth is ever expanding (Ripple et al. 2017), and the wildlife–livestock interface will likely continue to gain relevance for a growing proportion of migratory species as components of their habitat face agricultural incursions. Within this context, negative interactions between wild species and nearby livestock are likely to increase (Gordon 2018), with disease transfer risks providing just one example. Further, the unprecedented rate of species domestication for aquaculture, in particular (Duarte et al. 2007), and a suite of other risk factors for disease transfer in the marine environment (Krkossek 2017), mean that the marine wildlife–livestock interface will likely remain a hotspot for infectious disease in migratory marine species and a focal point for future research.

Migratory species are particularly difficult to conserve, given that they rely on multiple connected but geographically distinct habitat regions (Runge et al. 2014). Despite optimistic examples of conserving migratory corridors (Purdon et al. 2018; Chester and Hiltz 2019), maintaining adequate connected habitat remains a challenge, even in the wealthiest countries (Berger et al. 2014). While not a physical barrier to movement, infectious diseases from livestock could pose similar challenges for obligate migratory species, reducing the proportion of a population able to successfully migrate. Species would have to adapt (e.g., immunologically, phenologically, or behaviourally) or perish. For ocean-run sockeye salmon, to use our focal example, adaptation could be possible, since the species has repeatedly evolved a landlocked form (kokanee; Wood et al. 2008), and a small proportion of Fraser River sockeye already use a less salmon farm-exposed southern migration route (Tucker et al. 2009; Morton and Routledge 2016). Many other species might not be so lucky (Hardesty-Moore et al. 2018). For those species that evolved migration strategies in response to disease pressure, migration barriers — disease-induced or otherwise imposed — could even trap populations in the same maladaptive scenarios they originally evolved to evade (Satterfield et al. 2015).

If migration — clearly an adaptive strategy prior to human interventions — is to persist, we must ensure the necessary integrity of all components of migratory species’ requisite habitats. Much greater precaution and coordinated action will almost certainly be necessary (Mason et al. 2020).

Acknowledgements

We are very grateful to the Pacific Salmon Foundation and Genome British Columbia for funding and support to carry out the Strategic Salmon Health Initiative, the overarching program under which this study operated. This program was further part of the Salish Sea Marine Survival Project, led by the Pacific Salmon Foundation under the scientific leadership of Brian Riddell and Isobel Pearsall. MK is grateful for an NSERC Discovery Grant, Accelerator Award, and Canada Research Chair. Thanks to Marc Trudel, Chrys Neville, Jackie King, and the Hakai Juvenile Salmon Program for providing samples. Thanks also to Mark Lewis, Marie Auger-Méthé, Brendan Connors, and Cameron Freshwater for discussions at early stages of this analysis.

References

- Akaike, H. 1973. Information theory and an extension of the maximum likelihood principle. In Second International Symposium on Information Theory. Edited by B.N. Petrov and F. Csaki. Akadémiai Kiadó, Budapest. pp. 268–281.
- Altizer, S., Bartel, R., and Han, B.A. 2011. Animal migration and infectious disease risk. *Science*, **331**: 296–302. doi:[10.1126/science.1194694](https://doi.org/10.1126/science.1194694). PMID:[21252339](https://pubmed.ncbi.nlm.nih.gov/21252339/).
- Avendaño-Herrera, R., Toranzo, A., and Magariños, B. 2006. Tenacibaculosis infection in marine fish caused by *Tenacibaculum maritimum*: a review. *Dis. Aquat. Org.*, **71**: 255–266. doi:[10.3354/dao071255](https://doi.org/10.3354/dao071255). PMID:[17058606](https://pubmed.ncbi.nlm.nih.gov/17058606/).
- Bakke, T.A., and Harris, P.D. 1998. Diseases and parasites in wild Atlantic salmon (*Salmo salar*) populations. *Can. J. Fish. Aquat. Sci.*, **55**(S1): 247. doi:[10.1139/d98-021](https://doi.org/10.1139/d98-021).
- Bass, A.L., Stevenson, C.F., Porter, A.D., Rechisky, E.L., Furey, N.B., Healy, S.J., et al. 2020. In situ experimental evaluation of tag burden and gill biopsy reveals survival impacts on migrating juvenile sockeye salmon. *Can. J. Fish. Aquat. Sci.*, **77**(12): 1865–1869. doi:[10.1139/cjfas-2020-0134](https://doi.org/10.1139/cjfas-2020-0134).
- Bateman, A.W., Schulze, A.D., Kaukinen, K.H., Tabata, A., Mordecai, G., Flynn, K., et al. 2021. Descriptive multi-agent epidemiology via molecular screening on Atlantic salmon farms in the Northeast Pacific Ocean. *Sci. Rep.*, **11**: 3466. doi:[10.1038/s41598-020-78978-9](https://doi.org/10.1038/s41598-020-78978-9). PMID:[33568681](https://pubmed.ncbi.nlm.nih.gov/33568681/).
- Beacham, T.D., Lapointe, M., Candy, J.R., McIntosh, B., MacConnachie, C., Tabata, A., et al. 2004. Stock identification of Fraser River sockeye salmon using microsatellites and major histocompatibility complex variation. *Trans. Am. Fish. Soc.*, **133**: 1117–1137. doi:[10.1577/T04-0011](https://doi.org/10.1577/T04-0011).
- Beacham, T.D., McIntosh, B., and Wallace, C. 2010. A comparison of stock and individual identification for sockeye salmon (*Oncorhynchus nerka*) in British Columbia provided by microsatellites and single nucleotide polymorphisms. *Can. J. Fish. Aquat. Sci.*, **67**(8): 1274–1290. doi:[10.1139/F10-061](https://doi.org/10.1139/F10-061).
- Bengis, R.G., Kock, R.A., and Fisher, J. 2002. Infectious animal diseases: the wildlife/livestock interface. *Rev. Sci. Tech.*, **21**: 53–65. doi:[10.20506/rst.21.11322](https://doi.org/10.20506/rst.21.11322). PMID:[11974630](https://pubmed.ncbi.nlm.nih.gov/11974630/).
- Berger, J., Cain, S.L., Cheng, E., Dratch, P., Ellison, K., Francis, J., et al. 2014. Optimism and Challenge for Science-Based Conservation of Migratory Species in and out of U.S. National Parks: Conservation Action for Migratory Species. *Conserv. Biol.*, **28**: 4–12. doi:[10.1111/cobi.12235](https://doi.org/10.1111/cobi.12235). PMID:[24400726](https://pubmed.ncbi.nlm.nih.gov/24400726/).
- Bolker, B.M. 2008. Ecological models and data in R. Princeton University Press, Princeton, N.J.
- Burnham, K.P., and Anderson, D.R. 2002. Model selection and multimodel inference: a practical information-theoretic approach. Springer Verlag, New York.
- Chandler, P., Foreman, M.G.G., Ouellet, M., Mimeaule, C., and Wade, J. 2017. Oceanographic and environmental conditions in the Discovery Islands, British Columbia. *Fisheries and Oceans Canada*.
- Chester, C.C., and Hiltz, J.A. 2019. The Yellowstone to Yukon Conservation Initiative as an adaptive response to climate change. In *Handbook of climate change and biodiversity*. Springer. pp. 179–193.
- Cohen, B.I. 2012. The uncertain future of Fraser River sockeye. *Commission of Inquiry into the Decline of Sockeye Salmon in the Fraser River (Canada)*. Commission of Inquiry into the Decline of Sockeye Salmon in the Fraser River, Vancouver, B.C.
- Connors, B.M., Braun, D.C., Peterman, R.M., Cooper, A.B., Reynolds, J.D., Dill, L.M., et al. 2012. Migration links ocean-scale competition and local ocean conditions with exposure to farmed salmon to shape wild salmon dynamics. *Conserv. Lett.*, **5**: 304–312. doi:[10.1111/j.1755-263X.2012.00244.x](https://doi.org/10.1111/j.1755-263X.2012.00244.x).
- COSEWIC. 2017. COSEWIC assessment and status report on the sockeye salmon, *Oncorhynchus nerka*, 24 designatable units in the Fraser River drainage basin, in Canada. Committee on the Status of Endangered Wildlife in Canada, Ottawa, Ont.
- Costello, M.J. 2009. The global economic cost of sea lice to the salmonid farming industry. *J. Fish Dis.*, **32**: 115–118. doi:[10.1111/j.1365-2761.2008.01011.x](https://doi.org/10.1111/j.1365-2761.2008.01011.x). PMID:[19245636](https://pubmed.ncbi.nlm.nih.gov/19245636/).
- Csardi, G., and Nepusz, T. 2006. The igraph software package for complex network research. *InterJournal, Complex Systems*, **1695**: 1–9.
- de Castro, F., and Bolker, B. 2004. Mechanisms of disease-induced extinction. *Ecol. Lett.*, **8**: 117–126. doi:[10.1111/j.1461-0248.2004.00693.x](https://doi.org/10.1111/j.1461-0248.2004.00693.x).

- marine behavior and survival of migrating juvenile Sockeye Salmon. Trans. Am. Fish. Soc. **148**: 636–651. doi:[10.1002/tafs.10156](https://doi.org/10.1002/tafs.10156).
- Taranger, G.L., Karlsen, Ø., Bannister, R.J., Glover, K.A., Husa, V., Karlsbakk, E., et al. 2015. Risk assessment of the environmental impact of Norwegian Atlantic salmon farming. ICES J. Mar. Sci. **72**: 997–1021. doi:[10.1093/icesjms/fsu132](https://doi.org/10.1093/icesjms/fsu132).
- Thakur, K.K., Vanderstichel, R., Li, S., Laurin, E., Tucker, S., Neville, C., et al. 2018. A comparison of infectious agents between hatchery-enhanced and wild out-migrating juvenile chinook salmon (*Oncorhynchus tshawytscha*) from Cowichan River, British Columbia. FACETS, **3**(1): 695–721. doi:[10.1139/facets-2017-0113](https://doi.org/10.1139/facets-2017-0113).
- Tucker, S., Trudel, M., Welch, D.W., Candy, J.R., Morris, J.F.T., Thiess, M.E., et al. 2009. Seasonal stock-specific migrations of juvenile sockeye salmon along the West Coast of North America: Implications for Growth. Trans. Am. Fish. Soc. **138**: 1458–1480. doi:[10.1577/T08-2111](https://doi.org/10.1577/T08-2111).
- Vollset, K.W., Krontveit, R.I., Jansen, P.A., Finstad, B., Barlaup, B.T., Skilbrei, O.T., et al. 2016. Impacts of parasites on marine survival of Atlantic salmon: a meta-analysis. Fish Fish. **17**: 714–730. doi:[10.1111/faf.12141](https://doi.org/10.1111/faf.12141).
- Welch, D.W., Melnychuk, M.C., Payne, J.C., Rechisky, E.L., Porter, A.D., Jackson, G.D., et al. 2011. In situ measurement of coastal ocean movements and survival of juvenile Pacific salmon. Proc. Natl. Acad. Sci. U.S.A. **108**: 8708–8713. doi:[10.1073/pnas.1014044108](https://doi.org/10.1073/pnas.1014044108). PMID:21558442.
- Wiethoelter, A.K., Beltrán-Alcrudo, D., Kock, R., and Mor, S.M. 2015. Global trends in infectious diseases at the wildlife–livestock interface. Proc. Natl. Acad. Sci. U.S.A. **112**: 9662–9667. doi:[10.1073/pnas.1422741112](https://doi.org/10.1073/pnas.1422741112). PMID:26195733.
- Wood, C.C., Bickham, J.W., Nelson, R.J., Foote, C.J., and Patton, J.C. 2008. Recurrent evolution of life history ecotypes in sockeye salmon: implications for conservation and future evolution: Recurrent evolution of ecotypes in sockeye salmon. Evol. Appl. **1**: 207–221. doi:[10.1111/j.1752-4571.2008.00028.x](https://doi.org/10.1111/j.1752-4571.2008.00028.x). PMID:25567627.

Appendix A

Figures A2–A7 and Table A1 appear on the following pages.

Additional model forms

The advection–diffusion–decay susceptible-only model (used for tuning the spatial component of the model) took the following form:

$$(A1) \quad \frac{\partial S(x, t)}{\partial t} = D \frac{\partial^2 S(x, t)}{\partial x^2} - \frac{\partial v(x)S(x, t)}{\partial x} + f(x, t) - \mu S(x, t)$$

The SEIR version of the model described in the main text takes the following form:

$$(A2A) \quad \frac{\partial S}{\partial t} = D \frac{\partial^2 S}{\partial x^2} - \frac{\partial v S}{\partial x} + f - \mu S - S\phi$$

$$(A2B) \quad \frac{\partial E}{\partial t} = D \frac{\partial^2 E}{\partial x^2} - \frac{\partial v E}{\partial x} + S\phi - \mu E - \rho E$$

$$(A2C) \quad \frac{\partial I}{\partial t} = D \frac{\partial^2 I}{\partial x^2} - \frac{\partial v I}{\partial x} + \rho E - \mu_I I - \gamma I$$

$$(A2D) \quad \frac{\partial R}{\partial t} = D \frac{\partial^2 R}{\partial x^2} - \frac{\partial v R}{\partial x} + \gamma I - \mu R$$

Uncertainty

A likelihood profile for a single parameter can be generated by fixing the parameter of interest at a sequence of relevant values and, for each, minimising the model's “restricted” negative log-likelihood across the remaining free parameters. Twice the difference between the minimum value of the restricted negative log likelihood and the overall minimum negative log likelihood is asymptotically χ^2 -distributed with one degree of freedom, allowing a confidence interval to be generated from the likelihood profile (e.g., Bolker 2008). The same process can be used to generate multidimensional likelihood profiles, and associated confidence regions, with χ^2 degrees of freedom equal to the number of restricted parameters.

Fig. A1. Model-output population density (A) and *Tenacibaculum maritimum* infection prevalence (B) in space and time. Darker regions indicate higher density or prevalence. Grey circles (area proportional to sample size) show sampling dates and locations for out-migrating Fraser River sockeye, and corresponding blue circles in panel B indicate sampled fish that tested positive for *T. maritimum*. [Colour online.]

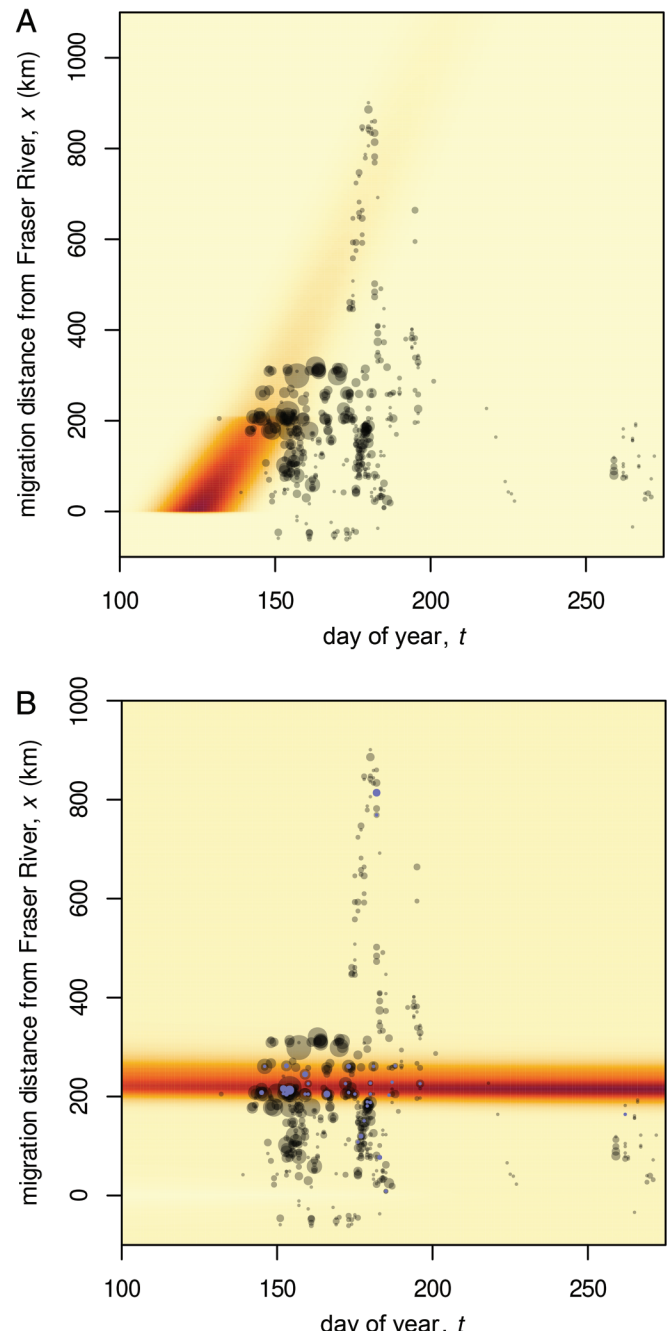


Table A1. Sockeye stocks analysed.

Sockeye stocks	Migration timing	Reference
Early Stuart, Rossette, Blackwater, Dust, Paula, Cayenne	Early Stuart	Neville et al. 2016
Bowron, Chilliwack, Dolly Varden, Fennel, Gates, Nadina, Nahatlatch, Pitt, Seymour, Scotch, Upper Adams	Early summer	Neville et al. 2016
Chilko, Kuzkwa Creek, Pinchi Creek, Middle River, North Thompson, Quesnel, Raft, Stellako, Tachie	Summer	Neville et al. 2016; COSEWIC 2017
Cultus, Big Silver, Birkenhead, Late Shuswap, Lower Shuswap, Little Shuswap, Weaver	Late	Neville et al. 2016; COSEWIC 2017

Fig. A2. Collection locations for sockeye salmon (blue dots), along their northwestward migration after marine entry at the Fraser River mouth (black triangle, lower right). Open red dots indicate molecular detections of *Tenacibaculum maritimum* in sockeye smolts. Black crosses show the locations of open-net salmon farms along the sockeye migration route (west coast Vancouver Island farms not shown). Dashed boxes indicate high-intensity salmon farming regions of the Broughton Archipelago and Discovery Islands. (Map data are from Environmental Reporting BC via the bcmath R package. Salmon farm locations are from DFO Aquaculture Management Division. Map projection is equirectangular.) [Colour online.]

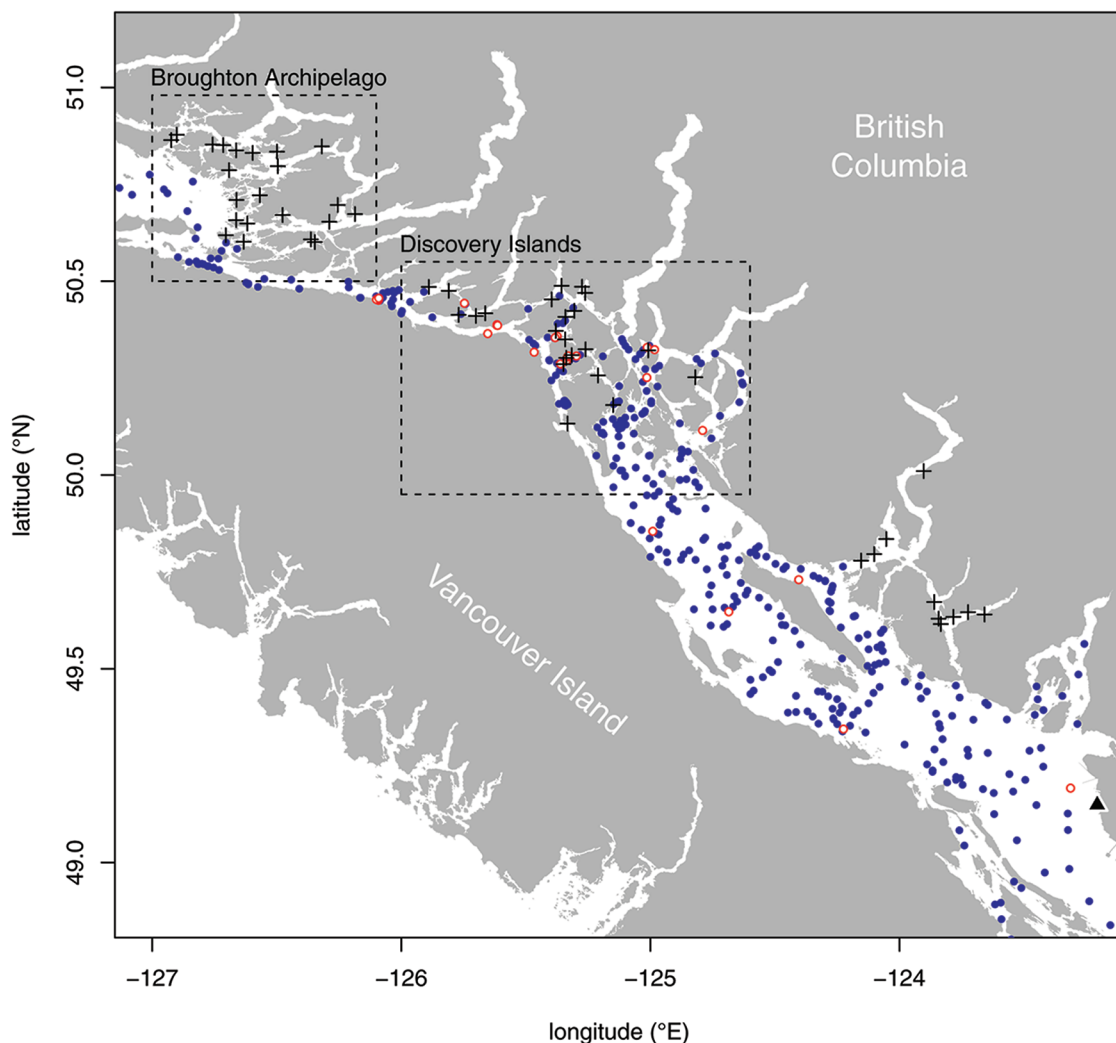


Fig. A3. Example of relationship between migration distance and seaway distance to the Sargeaunt Pass salmon farm, for sampled sockeye salmon. The red line segments represent a fitted absolute value model, with ordinate and abscissa shifts, and the shaded region represents 95% of the probability density associated with the normal distribution of model residuals. [Colour online.]

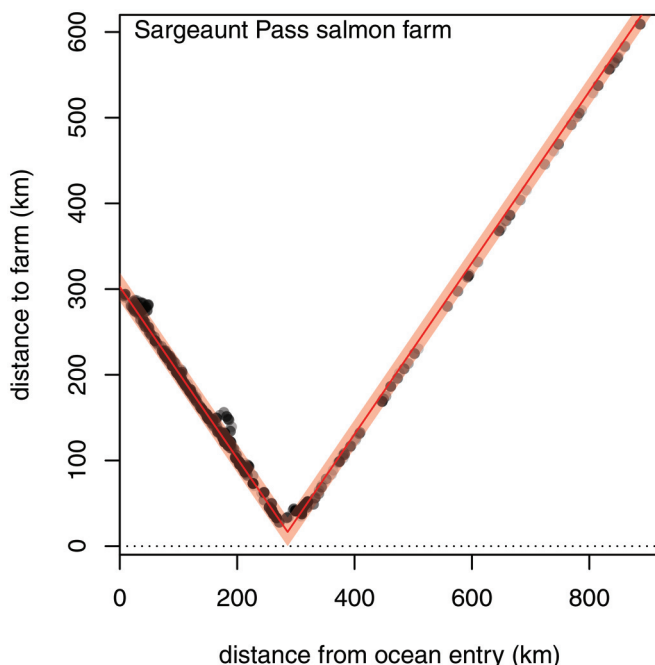


Fig. A4. Combined salmon farm-origin *Tenacibaculum maritimum* infection pressure in northwest-migrating Fraser River sockeye smolts for different values of the “spread” parameter, σ (standard deviation of single-farm Gaussian dispersal kernel). From lightest to darkest, plot shows σ equal to 50, 12.8 (dashed curve; 95% CI bound for the most parsimonious model in the main text), 5, 1 (solid curve, MLE value from the most parsimonious model), and 0.1. For illustration purposes, contributions from all farms are scaled by farm activity and do not vary by region. Estimates resulting from σ values of 1 and 0.1 almost completely overlap and are indistinguishable in the plot. “Rug” shows location of salmon farm tenures, with blue indicating Discovery Islands. [Colour online.]

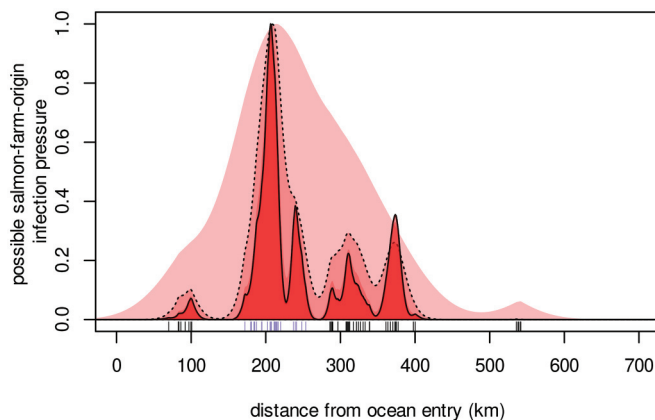


Fig. A5. Prevalence of *Tenacibaculum maritimum* infection in Fraser River sockeye salmon smolts migrating northwestward from the mouth of the Fraser River, BC ($x = 0$). Grey circles represent smolts caught in trawl surveys and purse-seine sampling between 2008 and 2018 (aggregated by location to illustrate pattern). Black curve shows predictions from a spatioepidemiological model of migration and infection dynamics, fitted to the prevalence data and plotted for the average ordinal day of fish capture. Red dashed lines show model-fit relative infection pressure from background and salmon farm-origin sources (scale arbitrary); weighting of infection pressure from Discovery Island farms, relative to farms from other regions, is fixed at 4.60 (the lower bound of the associated 95% confidence interval). “Rug” shows location of salmon farm tenures, with blue indicating Discovery Islands farms. [Colour online.]

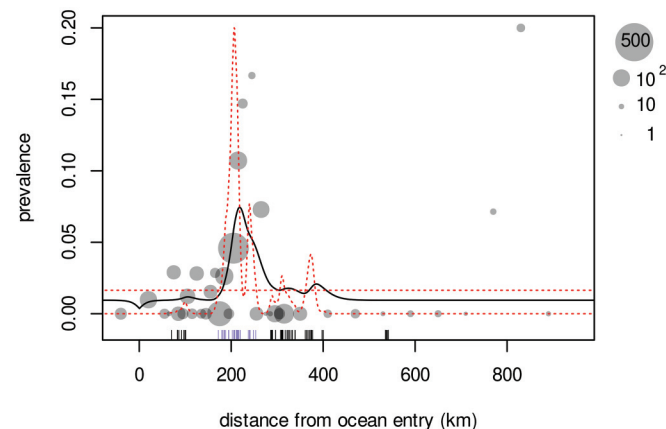


Fig. A6. Prevalence of *Tenacibaculum maritimum* infection in Fraser River sockeye salmon smolts migrating northwestward from the mouth of the Fraser River, BC ($x = 0$). Grey circles represent smolts caught in trawl surveys and purse-seine sampling between 2008 and 2018 (aggregated by location to illustrate pattern). Black curve shows predictions from a spatioepidemiological model of migration and infection dynamics, allowing for full recovery from infection, fitted to the prevalence data and plotted for the average ordinal day of fish capture. Red dashed lines show model-fit relative infection pressure from background and salmon farm-origin sources (scale arbitrary). “Rug” shows location of salmon farm tenures, with blue indicating Discovery Islands farms. [Colour online.]

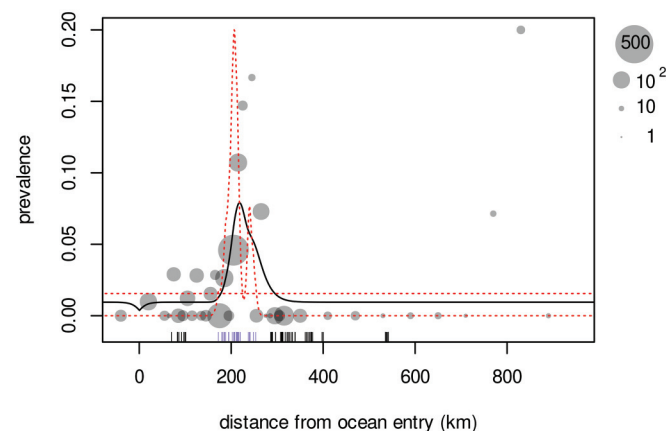


Fig. A7. Likelihood profiles-surfaces and confidence intervals-regions for key model parameters. (A) Likelihood profile for Discovery Island infection weighting exponent (δ ; solid curve), with dotted lines indicating 95% confidence interval (vertical) and associated critical likelihood value (horizontal). (B) Likelihood profile for standard deviation of farm-infection kernel (σ) with 95% confidence interval and critical likelihood value indicated as in panel A. (C) Two-dimensional likelihood surface infected mortality rate ($\mu_I = e^\eta \mu$; 0.00924 day^{-1} is baseline survival, μ) and infected recovery rate (γ). Yellow indicates lower values and contours indicates 95% (dotted) and 50% (dashed) confidence regions. Point shows maximum-likelihood parameter values (note log scale on mortality axis). (D) Likelihood surface for background infection rate (β_0) and maximum farm-source infection rate (β_F) with confidence regions and maximum-likelihood values indicated as in panel C; solid lines have slopes of 4.5 and 31. [Colour online.]

